

PAB and PEB Temperature Gradient Methodology for CAR Optimization

Thuc H. Dam, Andrew Jamieson, Maiying Lu, Ki-Ho Baik
Intel Mask Operations, 3065 Bowers Ave. Santa Clara, CA 95054;

ABSTRACT

Chemically amplified resist (CAR) performance can be greatly influenced by post apply bake (PAB) and post exposure bake (PEB) conditions. The difficulty with optimizing these conditions for photomask process is cost and time. In typical wafer CAR resist development, multiple wafer splits and skews can be rapidly processed with relatively low cost and fast turn around time, whereas in photomask processing each ebeam-written mask with a set of DOE conditions can be expensive and time consuming to produce.

This paper discusses a novel mask design and testing methodology that allow for many combinations of PEB and PAB conditions to be evaluated with one mask. In brief, this methodology employs orthogonal PAB and PEB thermal gradients across a plate. Some thermal profile, darkloss, resist top down critical dimensions (CD), and SEM cross section image results will be shared and discussed.

Keywords: Photomask, Coating, Resist, CAR, PAB, PEB

1. INTRODUCTION

As photomask requirements tighten with each succeeding generation, most mask making process parameters must be optimized to deliver required lithographic capabilities. PAB and PEB temperatures are two commonly optimized parameters for CARs as they can influence acid diffusion and kinetic reactions within a resist film which in turn can influence feature bias, resolution and linearity. A historical methodology that's been transplanted from wafer development is to use multi-plate design of experiment (DOE) where each wafer is baked with different combinations of PAB and PEB temperatures. Compared to wafer lithography development, mask development via multi-plate DOE is considerably more expensive and time consuming. This paper focuses on a novel mask design and comprehensive methodology for optimizing and understanding process windows for PAB and PEB parameters at a relatively inexpensive cost with rapid data return from a single mask.

The novel mask design will be discussed in detail with depictions of feature types and placement. The methodology of employing orthogonal PAB and PEB thermal gradients across a plate to effectively create a matrix of PAB and PEB temperatures will also be shown. Oven thermal data and indirect resist thickness measurements will be provided to demonstrate formation of thermal gradients, controlled thermal profile within each gradient, and the effects of thermal gradients on resist thickness. Finally CD metrics such as targetting, $\Delta CD/\Delta Dose$, linearity, and cross section data will be presented with respect to PAB and PEB window. This comprehensive technique hopefully will provide photomask resist lithographers with a cost effective and efficient toolset for gathering empirical data on PAB and PEB process windows for resist development.

2. EXPERIMENTAL

I. Test Plate Design

In order to fully exploit and extract pertinent data from orthogonally applied thermal gradients, a mask was design to be analyzed by top down SEM, scatterometry, and cross section SEM. The desired information to be captured by the design included resist CD resolution, linearity, bias, line width roughness (LWR), resist sidewall profile at multiple doses as a function of PEB and PAB. The design consisted of a basic unit (u) containing a SEM metrology cell, scatterometry cell, cross section cell. The SEM metrology cell contained isolated & nested lines, spaces, contacts, & pads with varying targets (50 – 1000 nm) and pitches (1:1 – 1:5). The scatterometry cell contained an array of nested

line/space, nested contacts, & nested pads with varying targets (100 – 300 nm) and pitches (1:1 – 1:3). The cross section cell contained isolated line, isolated space, nested l/s, nested contacts, and nested pads ranging from 50-1000 nm at 1:1 pitches.

The unit u was arrayed in 2×2 (U), where each unit u can be dosed differently. Each U was strategically arrayed across a mask with the unit center placed at thermal sensor locations (Figure 1).

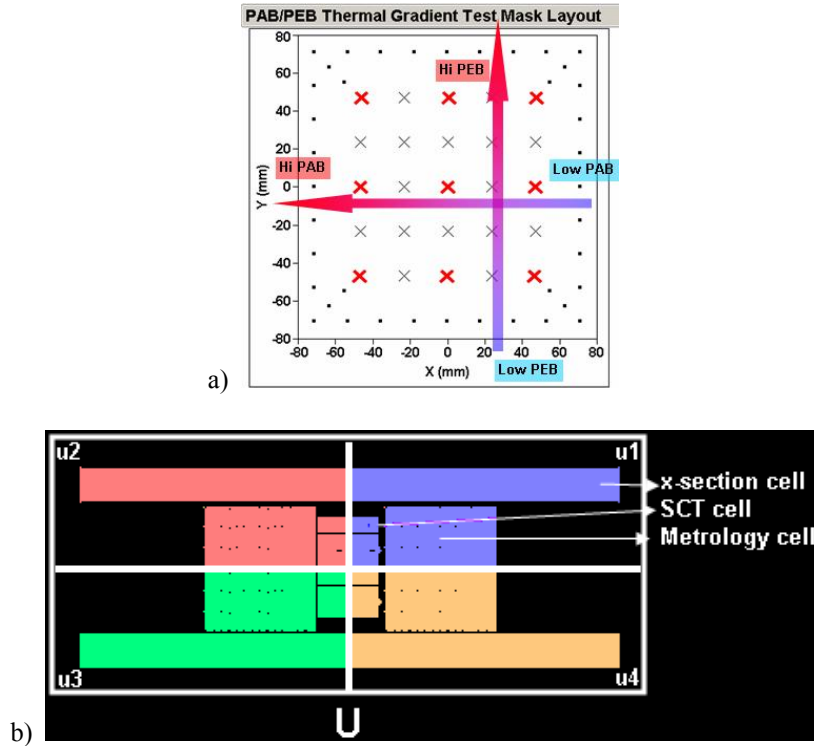


Figure 1. a) Top down physical layout of PAB/PEB gradient test mask. b) Unit cell depiction of metrology pattern that is placed at each marked location in (a).

II. Physical Design/Processing Methodology

Oven setup and tuning revolved around the use of advanced bake ovens where each thermal zone was tuned to induce a 10°C thermal gradient across a 6X6 inch mask substrate. PEB and PAB oven thermal gradients were verified with thermal sensor plate.

Once ovens were verified to have appropriate thermal profile, resist thickness verification was also performed to determine the impact of the thermal gradients on 4 coated photoblanks (unexposed), where the PAB and PEB conditions were matrixed as follows: PAB_{flat}/PEB_{flat} , $PAB_{gradient}/PEB_{flat}$, $PAB_{gradient}/PEB_{gradient}$, and $PAB_{flat}/PEB_{gradient}$. Each blank underwent the following process: coating with Resist A (a positive tone CAR), PAB, post-PAB resist thickness measurement, PEB, post-PEB resist thickness measurement, aqueous development, and post-developed resist thickness measurement. In each resist thickness measurement step, thickness data was collected at selected U locations on the coated blank using scatterometric technique. The applied 10°C thermal PAB and PEB gradients were always applied orthogonally to each other. PEB gradient was applied bottom to top, while PAB gradient was applied right to left (Figure 1a). The develop process used a standard aqueous 2.38% tetramethylammonium hydroxide (TMAH) develop chemistry.

Once oven thermal gradients were verified directly with thermal sensing plate and indirectly with resist thickness measurements, a single exposed mask was written on a blank that received a thermal PAB gradient, an orthogonal PEB

gradient, and aqueous development using same process as described above. In addition to the resist thickness measurements performed in between each process step, the developed mask received several resist-level CD measurements. These CD measurements included: 1) scatterometric measurements at all U locations, 2) CD SEM measurements at 3X3 matrixed U position (red x's in Figure1), and 3) cross section CD SEM measurements at 3X3 matrixed U position in center of the plate. The scatterometric measurements were collected on 100 and 200 nm, 1:1 nested lines/spaces, contacts, and pads at 5X5 matrixed U position (all x's in Figure 1). The CD SEM measurements were collected on 1) 100 and 200 nm 1:1 nested lines/spaces, contacts, and pads, 2) isolated/nested line linearity, 3) isolated/nest space linearity, 4) isolated/nested contact linearity, and 5) isolated/nested pad linearity. All isolated and 1:1 linearity data were collected on taped-features with sizes of 48, 60, 80, 100, 200, & 480 nm. Cross section SEM images were collected on isolated line, isolated space, 1:1 nested line/space, 1:1 nested contacts, and 1:1 nested pads for taped-features 150 nm down to smallest resolvable sizes in 10 nm increments.

3. RESULTS AND DISCUSSIONS

I. Thermal Results and Discussions

The key aspect of this paper was to set up controlled PEB and PAB thermal gradients across the plate. In order to verify that the gradients were properly set up, thermal sensor plates were used. In this proceeding section, absolute temperatures and bake times will not be disclosed, so all thermal data have been normalized to 0°C at the center point condition. As can be viewed in Figure 2a, a 10°C PAB thermal gradient was achieved from right (colder) to left (warmer) at ~500 seconds in the steady state region of bake time period, while Figure 2b depicts the thermal profile for the five horizontal points stretching across the middle of the plate. Figure 2c depicts this thermal data with respect to the plate's x-position, which showed a steady temperature was maintained along a single PAB thermal gradient.

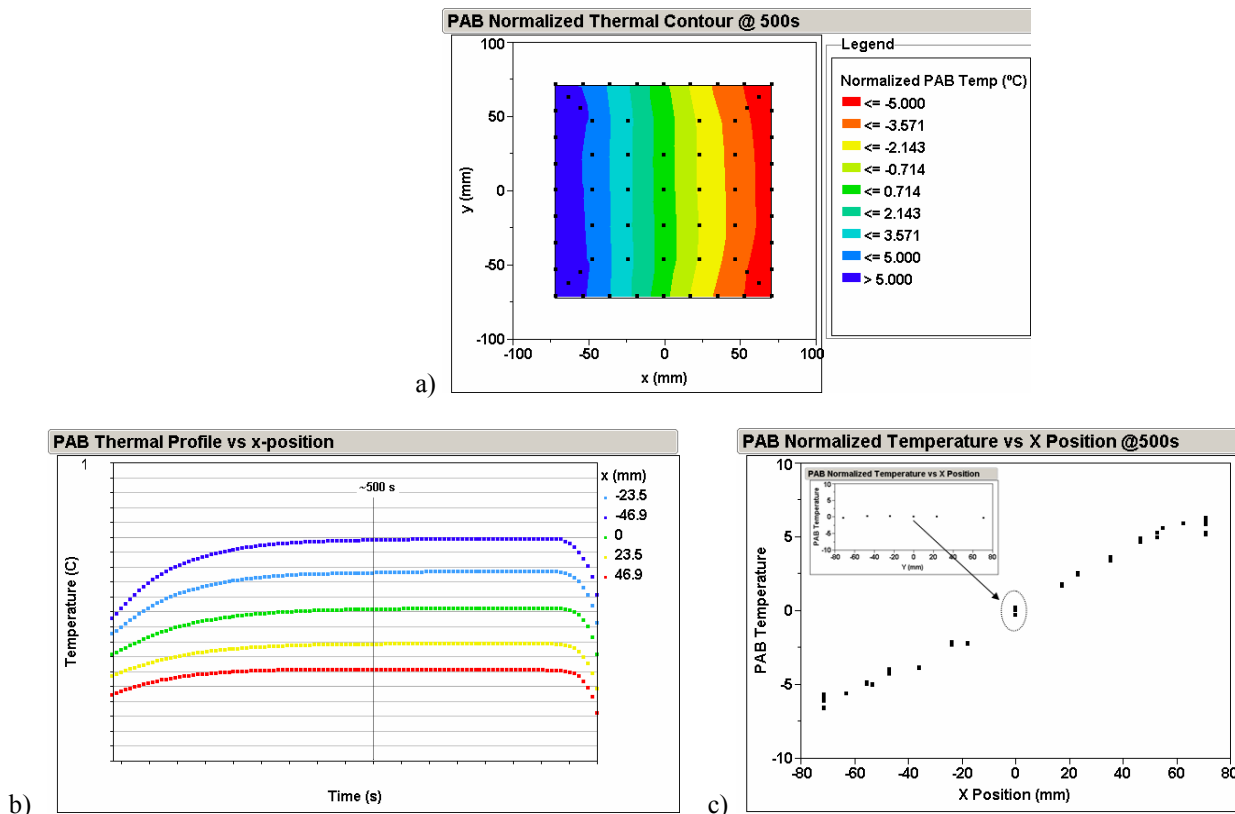


Figure 2. a) PAB thermal gradient contour. b) PAB thermal profile for 5 horizontal points stretching across middle of plates through different thermal gradients. c) PAB thermal data with respect to x-position across the mask.

As can be viewed in Figure 3a, a 15°C PEB thermal gradient was achieved from bottom (cooler) to top (warmer) at ~500 seconds in the steady state region of bake time period, while Figure 3b depicts the thermal profile for the four vertical points stretching across the middle of the plate. Figure 3c depicts this thermal data with respect to the plate's y-position, which showed a steady temperature was maintained along a single PEB thermal gradient.

The thermal data in the 5X5 center portion of the plate appears to be well controlled within each single gradient to less than 0.5°C variation, while temperatures across gradients are evenly spaced at about 2°C per gradient. These temperatures appear to be sufficiently spaced to detect CD movements relative to intended thermal temperature gradients. Also the thermal profile showed that maximum temperatures occurred during steady state period, so that the CD relationship can be directly correlated to steady state temperature and not to some overshoot temperature during baking.

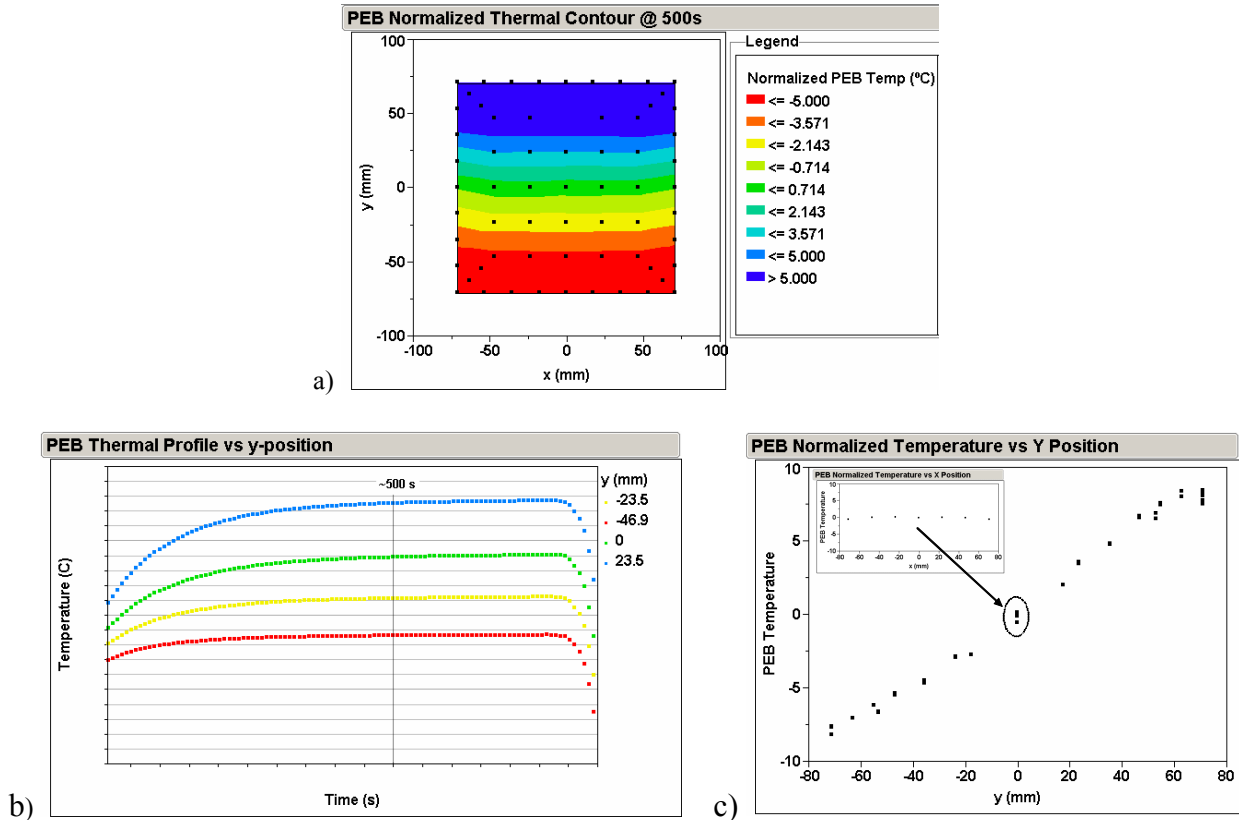


Figure 3. a) PEB thermal gradient contour. b) PEB thermal profile for 5 vertical points stretching across middle of plates through different thermal gradients. c) PEB thermal data with respect to y-position across the mask.

II. Resist Thickness Results and Discussions

The heating of thin resist film during PAB serves to remove residual casting solvent via evaporation and diffusion. This process can reduce a film's free volume and cause polymer compaction, which can impact CD through reduction of mean free path for acid diffusion during the PEB process.¹ Changes in resist film thickness can be measured indirectly to determine the relative applied temperature that a film received and the extent of compaction (acid mobility/permeability) of the film. The images in Figure 4 is a compilation of post-coat, post PAB resist thickness measurements for the matrix of coated blanks that were processed to indirectly confirm the PAB thermal gradients. During the application of PAB gradient, a resist-coated plate's left side was exposed to 10°C higher than its right side as discussed above, and the post coat resist thickness measurement in Figure 4a indicated that the left side of the plate was

thinner than the right side by $\sim 8 \text{ \AA}$ leading one to determine that Resist A had about 1 \AA of compaction per $^\circ\text{C}$ of PAB at the particular operating temperatures.

Although PEB serves a different purpose than PAB, it nevertheless is a heating process that could further compact a resist film, and again resist thickness measurement can be used to indirectly confirm the applied PEB thermal gradient. A coated plate that received a flat PAB and then a gradient PEB (10C higher at top of plate relative to bottom of plate) had thickness measurements indicating that the upper portion of the plate was $\sim 18 \text{ \AA}$ thinner than the bottom portion. This represented $\sim 1.5 \text{ \AA}$ of film compaction per $^\circ\text{C}$ of PEB. Both PAB and PEB thermal data correspond well with resist thickness data.

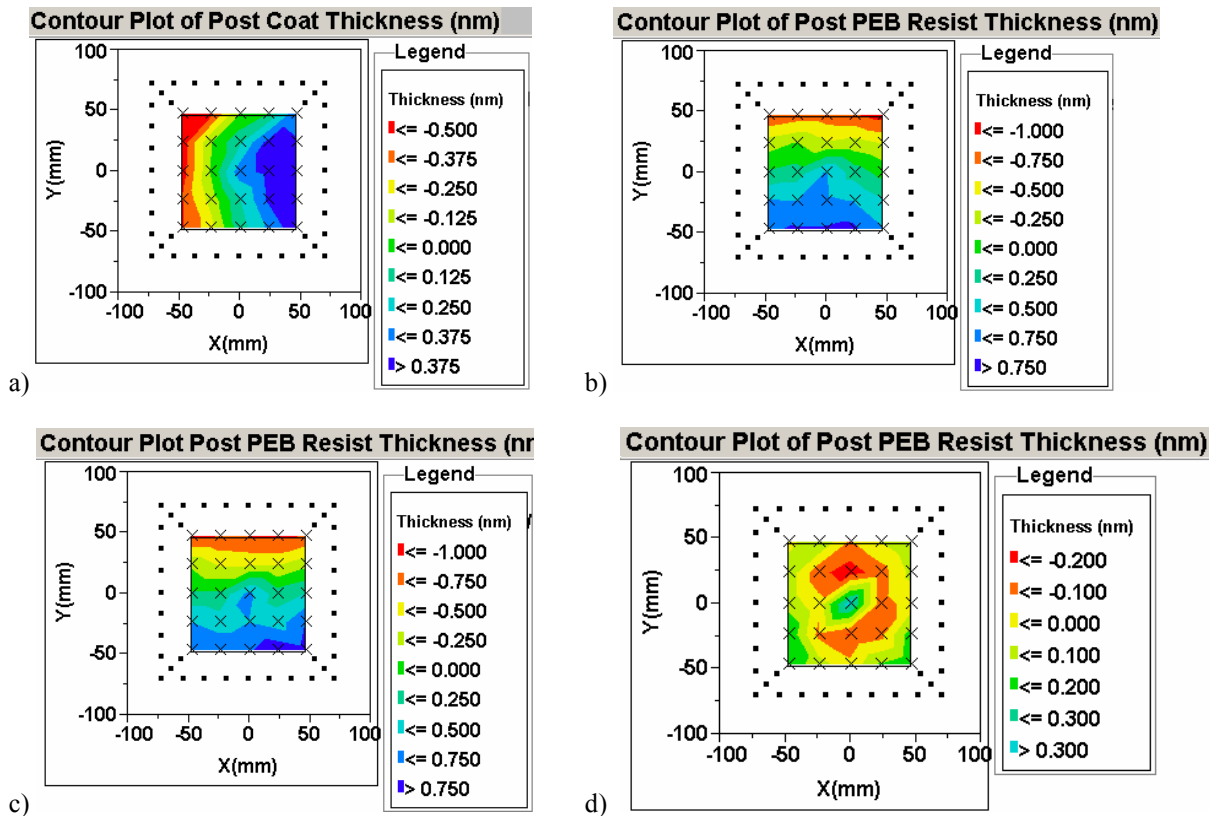


Figure 4. a) Post coat thickness of resist coated plate that received a gradient PAB. b) Post PEB thickness of a resist coated plate that received a flat PAB and then a gradient PEB. c) Post PEB thickness of a resist coated plate that received a gradient PAB and a gradient PEB. d) Post PEB thickness of a resist coated plate that received a flat PAB and a flat PEB (control).

A coated-plate that received PAB and PEB gradients applied orthogonally was also measured post PEB and post DEV. When orthogonal gradients were applied, the region of the plate that experienced the highest PAB and PEB temperature was the upper left corner and should have resulted in the thinnest resist film, while the coolest portion was the lower right corner and should have resulted in thickness resist film. However, experimental results at post PEB (Figure 4c) indicated a general resist thickness trend (thick at bottom, thin at top) that matched more with PEB thermal gradient (cool at bottom, hot at top), and led us to believe that resist thickness was more influenced by the last applied thermal condition, PEB.

Lastly a control plate was ran where a flat PAB and a flat PEB were applied, and its results indicated a 5 \AA radial resist thickness variation that could be attributable to the spin coating process or thermal radial profile from PEB or PAB ovens. This variation was less than the lateral thickness variation observed on the gradient baked plates.

PEB darkloss (post-PEB thickness – post-coat thickness) and DEV darkloss (post-develop thickness – post-PEB thickness) data were also monitored on the plates with the following PAB/PEB conditions: PAB_{flat}/PEB_{flat}, PAB_{gradient}/PEB_{flat}, PAB_{gradient}/PEB_{gradient}, and PAB_{flat}/PEB_{gradient}. Figure 5 shows PEB darkloss for all four cases, and indicates that hotter PAB tend to have less film compaction after PEB, while hotter PEB tend to have more film compaction post PEB. This phenomenon can potentially be explained in that the hotter PAB exposed region was already compacted/”hardened” so that subsequent PEB does not drive further film compaction, while the cooler PAB exposed region was not fully compacted so that subsequent PEB drove further observable film compaction.

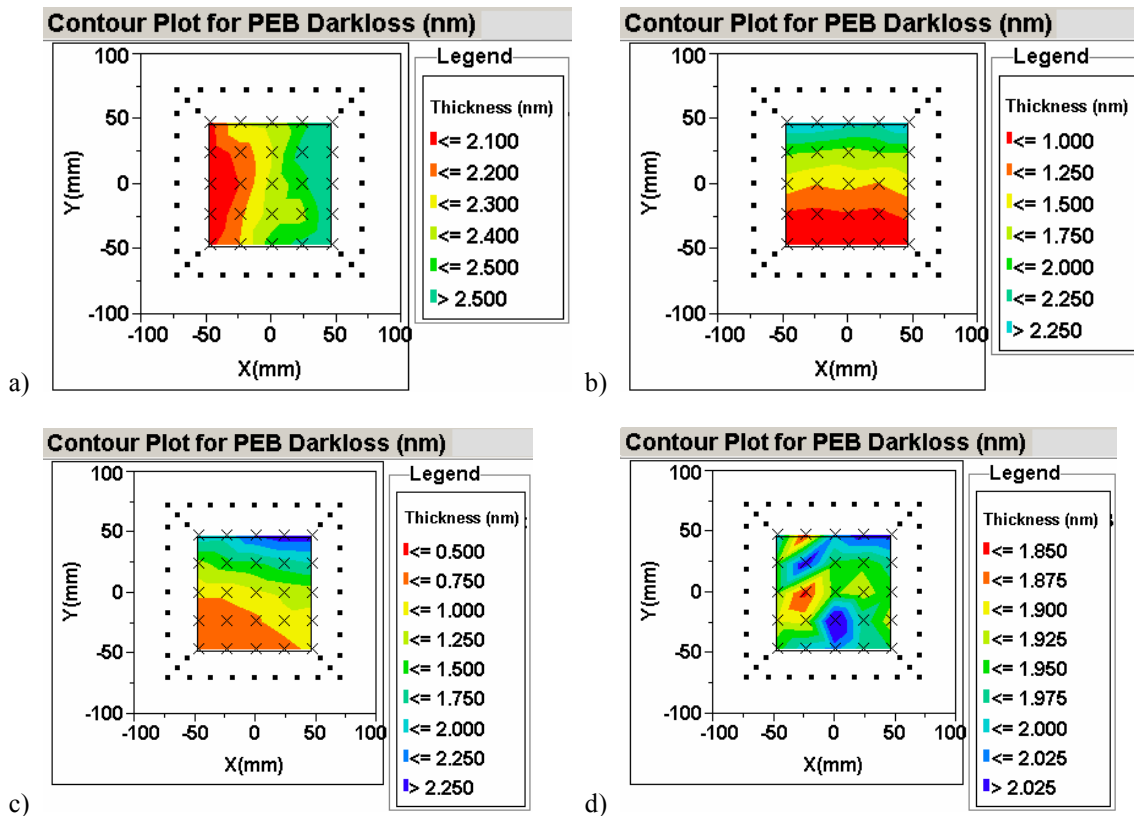


Figure 5. PEB darkloss for resist coated plates with a) PAB gradient/PEB flat, b) PAB flat/PEB gradient, c) PAB gradient/PEB gradient, and d) PAB flat/PEB flat (control).

III. Resist CD Results and Discussions

In this section, the CD results will be shared and discussed for a single patterned mask that was written on a blank that received a thermal PAB gradient, and orthogonal PEB gradient, and aqueous development. The plate design along with the PAB/PEB orthogonal gradients essentially allowed one to run a DOE with exposure dose, PAB temperature, and PAB temperatures as input parameters and various CD metrics as output responses. All data will be either from scatterometry or SEM. The scatterometry sampling is more robust covering the 5X5 portion of the mask (represented by all x's in Figure 1a). The SEM sampling is less robust and covers only the 3X3 portion of the mask (represented by only red x's in Figure 1a).

The first typical analysis that can be performed is a full factorial DOE to determine CD targetting relationship to the input parameters. In this example (Figure 6), 100 nm nested line features were measured on both SEM and scatterometry. From 6a and 6b, one can determine appropriate CD targetting and latitude as a function of dose, PEB temp, and PAB temp. One can also use this informaton to derive $\Delta CD/\Delta Dose$, $\Delta CD/\Delta PAB$, and $\Delta CD/\Delta PEB$. The

$\Delta CD/\Delta PEB$ and $\Delta CD/\Delta PAB$ were approximately $\leq 1 \text{ nm}/^\circ\text{C}$ and were fairly comparable between the the SEM and scatterometry data. $\Delta CD/\Delta Dose$ will be discussed in subsequent section.

Figures 6c & 6d are scatterometry and SEM contour plots, respectively, of 100 nm nested lines at one dose plotted as function of PAB and PEB temperatures. These two graphs help visually show CD response at a single dose as function of PAB/PEB gradients. Analyzing of this data showed that high PAB with high PEB led to larger nested lines (smaller spaces). Since Resist A is a positive tone CAR, one can possibly argue that high PAB/high PEB led to less acid diffusion that manifested in smaller space CD's (larger lines). This data point may be supported by the thinner resist film (high film compaction..less acid diffusion) at high PAB/high PEB (Figure 5c).

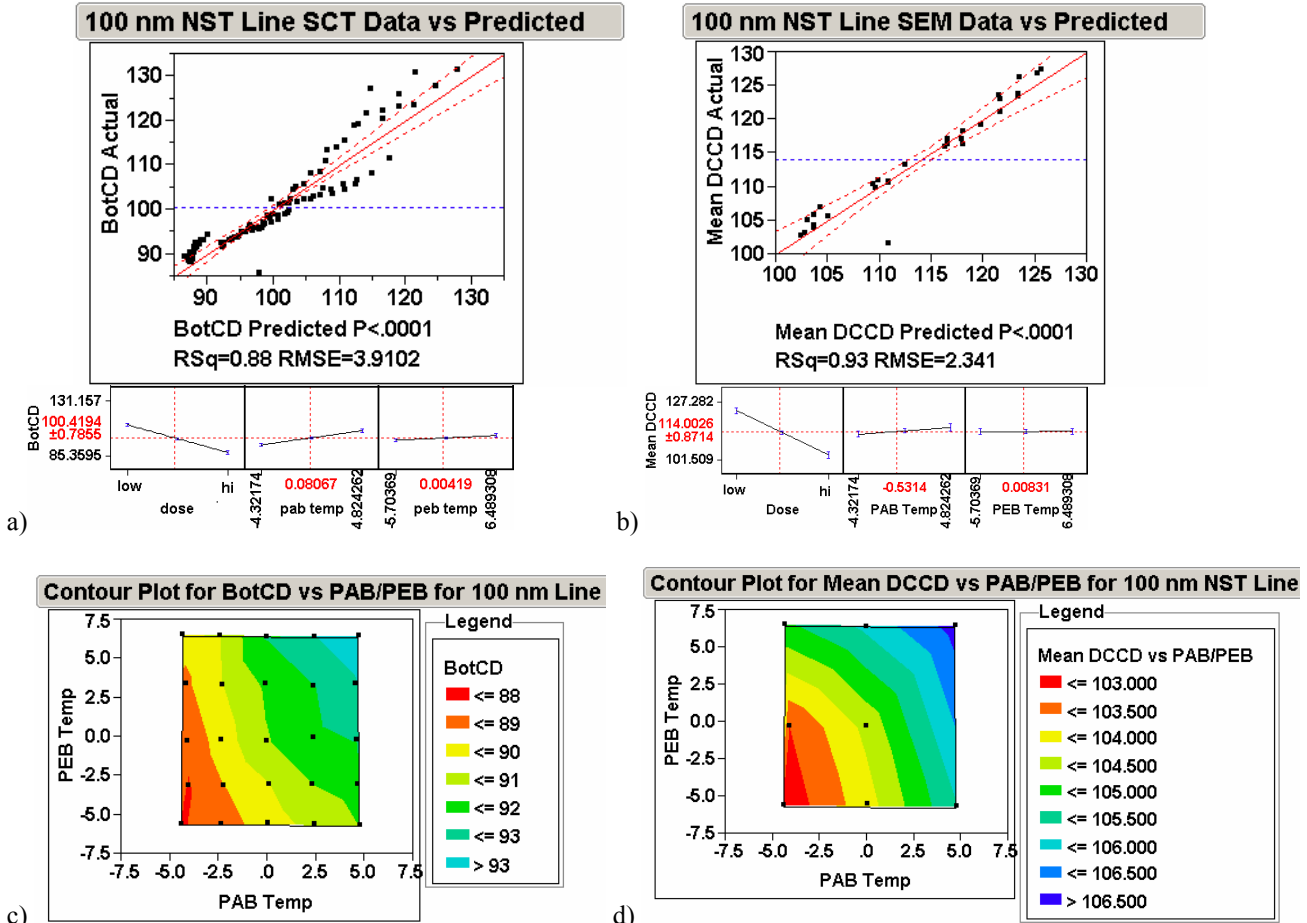


Figure 6. a) Scatterometry data for 100 nm nested lines vs. full factorial model prediction and its JMP prediction profiler. b) SEM data for 100 nm nested lines vs. full factorial model prediction and its JMP prediction profiler. c) Contour plot of scatterometry CD data of 100 nm nest line vs. PAB/PEB temperature. d) Contour plot of scatterometry CD data of 100 nm nest line vs. PAB/PEB temperature.

$\Delta CD/\Delta Dose$ as a function of PEB and PAB temperature is another more indepth CD analysis that one can also achieved with this plate design and test methology. For each thermal position (U) on this test plate, there are four different subunits (u) that can each be dosed differently (Figure 1). By measuring the same feature across different doses at each thermal position, $\Delta CD/\Delta Dose$ can be obtained for each PAB/PEB combination. A contour plot of $\Delta CD/\Delta Dose$ vs PAB & PEB can be generated to determine optimum PAB & PEB condition with respect to $\Delta CD/\Delta Dose$. The example provided in Figure 7a is scatterometry measurement of $\Delta CD/\Delta Dose$ of 200 nm nested lines. The contour results in Figure 7b indicate $\Delta CD/\Delta Dose$ is mostly influence by PAB gradient with little influence by PEB gradient. This data

along with resist thickness data may indicate that the lowered PAB baked portion of the mask has more residual solvent (thicker film) and allow for higher degree of acid diffusion during/after exposure but prior to PEB.

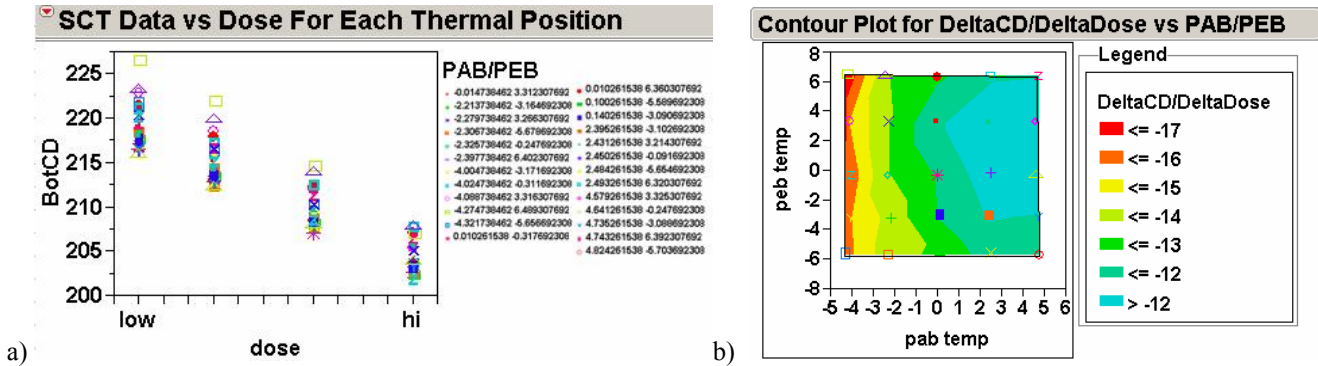


Figure 7. a) Scatterometry CD for 200 nm lines vs. dose for each PAB/PEB thermal combination. b) Δ CD/ Δ Dose contour as a function of PAB and PEB temperatures.

Linearity is another metric that can be assessed with this methodology. For instance, isolated contact linearity measurements can be gathered at each of the thermal positions and then plotted as a function of PAB and PEB temperatures (Figure 8). From this data, one could assume that lower PEB helps improve contact linearity performance, and that there seemed to be minimal influence from the PAB. The method for determining linearity values based on top-down CD measurements was semi-quantitative, and corroboration with top-down images and cross section could lead to better assessment of thermal contributions.

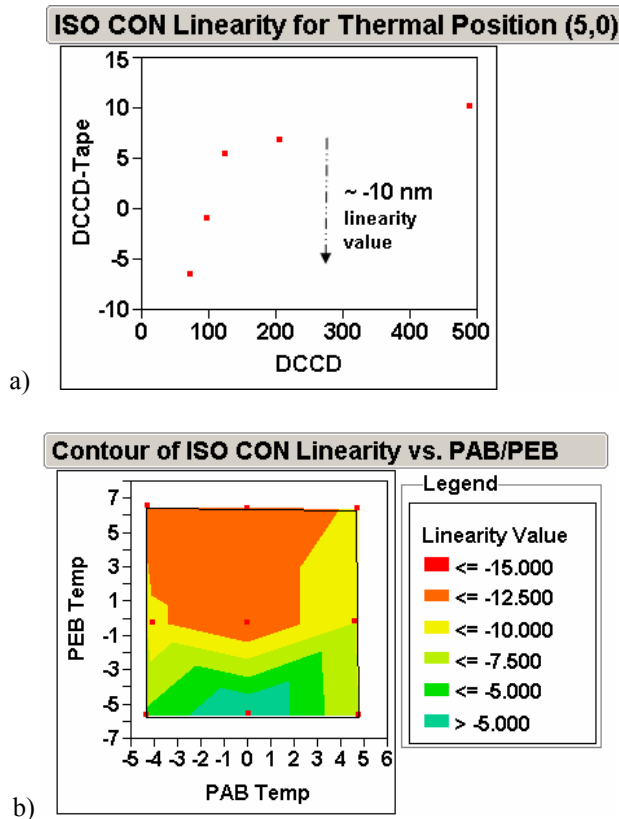


Figure 8. a) Isolated contact linearity graph for features placed at thermal position (5,0). b) Contour plot of isolated contact linearity values vs. PAB/PEB.

When isolated contact top-down images (Figure 9) were used to verify top-down CD measurements, it was difficult to discern that PAB or PEB had any influence on CD resolution or linearity. However cross section images for contacts (Figure 10) and cross section images for isolated spaces (Figure 11) demonstrated that resolution was improved with higher PEB (not lower PEB as assumed with top down CD measurements in Figure 8). Going through this exercise demonstrated that having multiple data perspectives could provide a more robust assessment, and having a thorough test mask design was instrumental for collecting data from multiple perspectives.

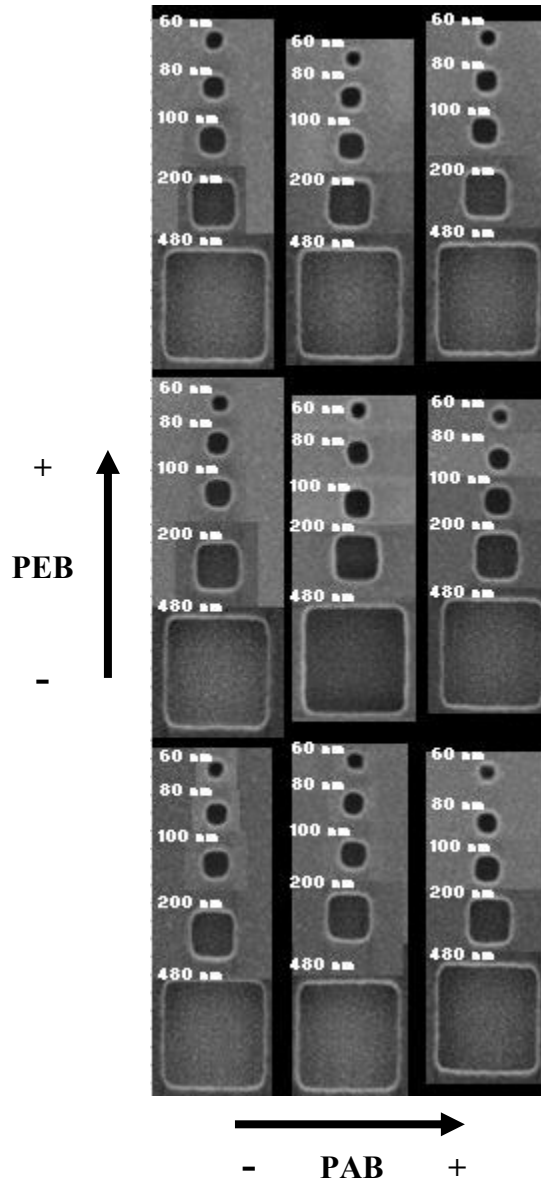


Figure 9. Isolated contact top-down SEM images vs. PAB/PEB.

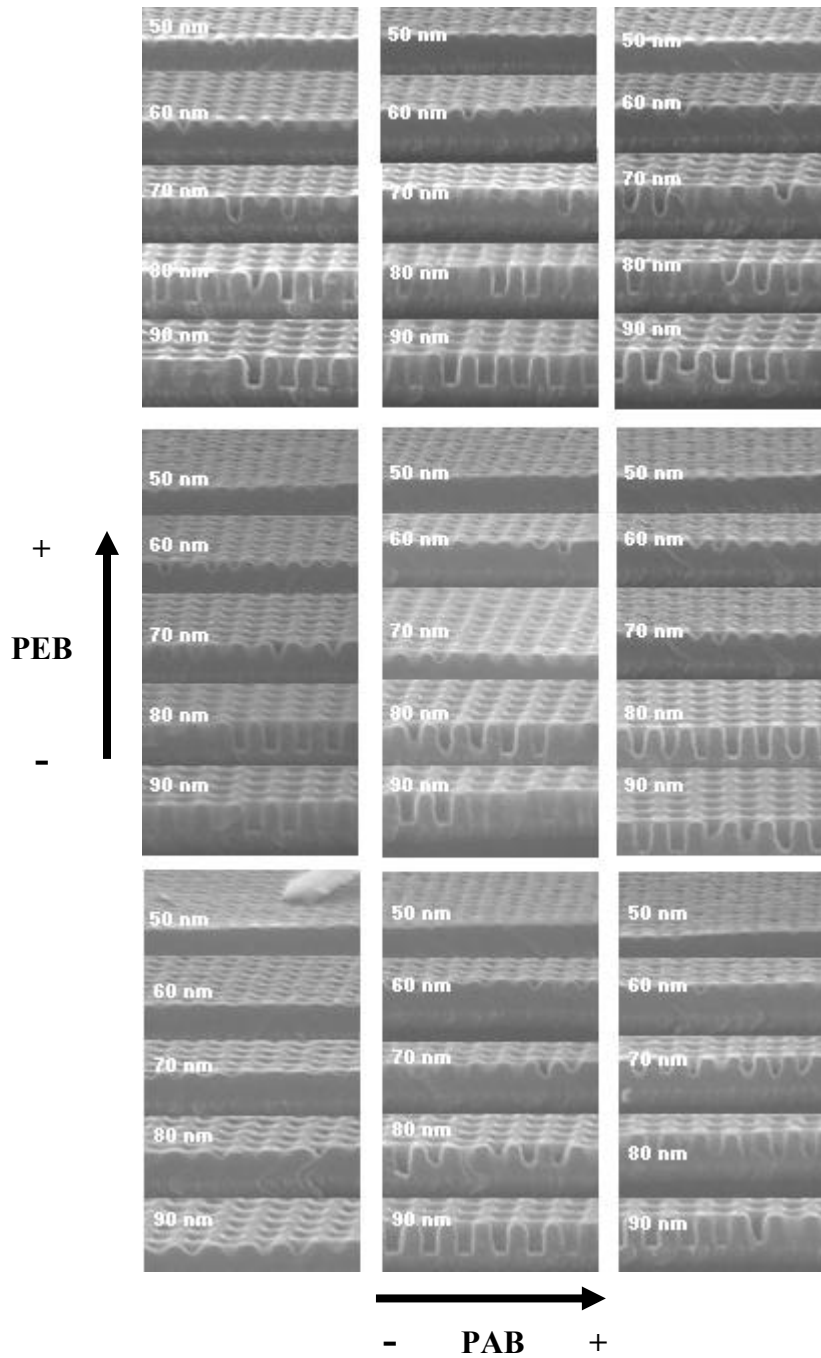


Figure 10. Nested contacts cross section SEM images vs. PAB/PEB.

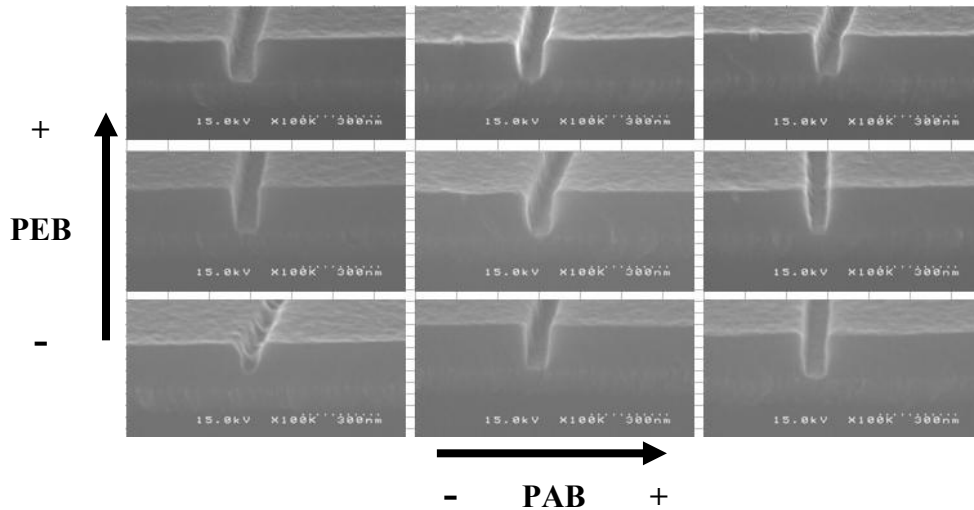


Figure 11. Isolated space cross section SEM images vs. PAB/PEB.

4. CONCLUSION

The key elements of using orthogonally applied PAB and PEB gradients to achieve thorough resist process development and characterization have been explained. The thermal and resist thickness/darkloss results demonstrated that thermal gradients were achieved in a highly controlled manner. From an analytical methodology perspective, CD responses such as targetting, $\Delta CD/\Delta Dose$, linearity, and cross section were collected and analyzed with respect to PAB and PEB. The methodology appears robust and thorough enough to assess a large amount of data from multiple perspectives. In summary, a cost effective/time efficient tool set and its analytical applications have been provided to help conduct comprehensive assessment of PAB and PEB's effects on resist CD's.

ACKNOWLEDGEMENTS

The author of this paper would like to acknowledge the support of Mark Nakahama for design layout & tapeout, Mario Azizi for collecting xsection SEM images, Max Lau & Tahir Naseer for creating SEM metrology job, and Kyung Lee for creating scatterometry job.

REFERENCES

1. J. Byers, M. Smith, and C. Mack, Modeling Soft Bak Effects in Chemically Amplified Resists, Proc SPIE vol 5039 (2003) pp 1143-1154.